

Dalton Transactions

Accepted Manuscript



This is an *Accepted Manuscript*, which has been through the Royal Society of Chemistry peer review process and has been accepted for publication.

Accepted Manuscripts are published online shortly after acceptance, before technical editing, formatting and proof reading. Using this free service, authors can make their results available to the community, in citable form, before we publish the edited article. We will replace this *Accepted Manuscript* with the edited and formatted *Advance Article* as soon as it is available.

You can find more information about *Accepted Manuscripts* in the [Information for Authors](#).

Please note that technical editing may introduce minor changes to the text and/or graphics, which may alter content. The journal's standard [Terms & Conditions](#) and the [Ethical guidelines](#) still apply. In no event shall the Royal Society of Chemistry be held responsible for any errors or omissions in this *Accepted Manuscript* or any consequences arising from the use of any information it contains.



Journal Name

ARTICLE

Synthesis of novel pyridyl containing phospholanes and their polynuclear luminescent copper (I) complexes.

e Received 00th January 20xx,
Accepted 00th January 20xx

DOI: 10.1039/x0xx00000x

www.rsc.org/

E.I. Musina,^{a,*} A.V. Shamsieva,^a I.D. Strel'nik,^{a,b} T.P. Gerasimova,^a D.B. Krivolapov,^a I.E. Kolesnikov,^c E.V. Grachova,^b S.P. Tunik,^b C. Bannwarth,^d S. Grimme,^d S.A. Katsyuba,^a A.A. Karasik^a and O.G. Sinyashin^a

A novel type of cyclic P,N-ligands – pyridyl containing phospholanes – has been synthesized by reaction of primary phosphines with 1,4-dichlorobutane in the superbasic medium in the moderate yield. A series of homo tetranuclear octahedral Cu₄L₄L₂, dinuclear tetrahedral Cu₂L₂L₃, and dinuclear “head-to-tail” Cu₂L₂L₂ luminescent complexes with these ligands were obtained. All the compounds were characterized by a range of spectroscopic and computational techniques and, in the case of some Cu₄L₄L₂ and Cu₂L₂L₃ complexes, by single crystal X-ray diffraction. Structural diversity of the obtained complexes is reflected in their photophysical properties: phosphorescence spectra of the compounds display emission in broad spectral range of 471 – 615 nm. TD-DFT computations allow to assign the single emission band around 550 nm for Cu₂L₂L₃ complexes and 471 nm for Cu₂L₂L₂ complex to a vertical triplet-singlet transition from a metal-to-ligand and halide-to-ligand charge-transfer ³(M+X)LCT excited state, whereas a second band around 600 nm in the spectra of octahedral Cu₄L₄L₂ complexes is assigned predominantly to Cu₄L₄ cluster-centered (³CC) excited state.

Introduction

Phosphine complexes of copper(I) attracted considerable attention within the last decade as alternative base for novel luminescent materials.¹ In order to enhance photophysical characteristics of the complexes π -conjugated N-heterocycles, e.g. substituted bipyridines or pyridyl containing di-, tri- and tetrazoles, were used as chelating co-ligands.² Hybrid phosphinopyridines and related ligands are of special interest due to the presence of a photochromic N-heterocycle, incorporation of soft and hard donor centers in a relatively rigid molecular skeleton and their ability to stabilize various binuclear and tetranuclear complexes. Phosphinopyridines serve as P-monodentate, P,N-chelate or P,N-bridge ligands forming binuclear “head-to-tail”³ and “butterfly”⁴ cores, as well as tetranuclear cubane-like cores.⁵ It has been shown that increased structural rigidity reduces radiationless deactivation pathways in mononuclear copper(I) complexes and clusters leading

to strongly enhanced quantum yields.^{4a,6} A number of compounds with promising photophysical characteristics have been found up today. In particular, new Cu(I) dimers with diphenylphosphino-Pyridine ligands are shown to be the efficient thermally activated delayed fluorescence (TADF) emitters giving relatively short TADF decay times at ambient temperature and thus, represent good candidates for organic light-emitting diodes (OLED) applications.³ Most commonly, the highest occupied molecular orbital (HOMO) has a dominant metal d(Cu) character, probably mixed with some contribution of the phosphino group, while the lowest unoccupied molecular orbital (LUMO) is basically resident on the imine part of the hybrid ligand. Thus, the emission corresponding to the lowest triplet excited state is essentially ascribed to the metal-to-ligand charge transfer excited state which is normally sensitive to the coordination environment and structure of the ligand. This makes the emission spectrum easily tunable and a color spectrum ranging from blue to red has been covered with these types of compounds.^{4b} So, the photophysical properties of the complexes depend distinctly on the substitution pattern at the pyridine and phosphine moieties.^{4a} However, most of the studied copper complexes of phosphinopyridines contain only diphenylphosphino groups as phosphine moiety. In the present paper we report on the synthesis of novel phosphinopyridines containing a phospholane unit as phosphine part, their coordination ability towards copper iodide, as well as photochemical properties of the corresponding di- and tetranuclear copper(I) complexes.

^aA.E. Arbusov Institute of Organic and Physical Chemistry, Kazan Scientific Centre of the Russian Academy of Sciences, Arbuzov str. 8, 420088 Kazan, Russia, elli@iopc.ru

^bSt. Petersburg State University, Institute of Chemistry, Universitetskii pr. 26, 198504 St Petersburg, Russia

^cCenter for optical and laser materials research, Research park of St. Petersburg State University, Ulianovskaya St. 5, 198504 St. Petersburg, Russia

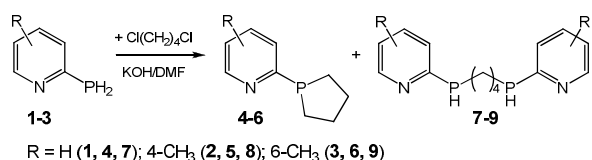
^dMulliken Center for Theoretical Chemistry, Institut für Physikalische und Theoretische Chemie der Universität Bonn, Beringstr. 4, 53115 Bonn, Germany.

† Electronic Supplementary Information (ESI) available: X-Ray molecular structure of complexes **13**; generated in ORTEP pictures of molecular structures of **10** and **12** with ellipsoids, optimized structure of complex **14**; calculated absorption spectra of compounds **4**, **10-14**; schematic representation of the molecular orbitals for the singlet ground state of **4** and **12**. See DOI: 10.1039/x0xx00000x

Results and discussion

Synthesis of P,N-Type Ligands. The phospholane was first synthesized one century ago⁷ by the reaction of the corresponding $\text{BrMg}(\text{CH}_2)_4\text{MgBr}$ with PhPCl_2 , and more recently⁸ phenylphospholane has been made by intramolecular ring closure reactions of $\text{PhP}(\text{H})(\text{CH}_2)_2\text{CH}=\text{CH}_2$. The *tert*-butyl- and phenylphospholane have been previously obtained by substitution reactions of $t\text{BuPCl}_2$ ⁹ or $\text{R}(\text{OMe})_2$ ($\text{R} = t\text{Bu}, \text{Ph}$)¹⁰ with dilithiated butane. These one-pot syntheses are convenient, and pure products are readily obtained, but the yields are at best modest. A modern approach to the synthesis of phospholane ring systems employs the reaction of lithium phosphide anions (derived from deprotonation of primary phosphines) with symmetrical cyclic sulfates (derived from corresponding 1,4-diols). Vedejs has reported the utilization of this approach to the synthesis of P-chirogenic monophospholanes from unsymmetrical cyclic sulfates.¹¹ Another approach is based on the reduction of multistep obtained P-oxide phospholane.¹²

The basic idea for our synthetic route has been developed from the synthetic procedure of Issleib who used the dilithium phosphide and 1,4-dihalogenbutane for the generation of phenyl, ethyl and cyclohexyl phospholanes in the yields of 20-30%.¹³ A novel pyridyl containing phospholanes **4-6** were obtained by interaction of corresponding primary phosphines **1-3** and 1,4-dichlorobutane in superbasic medium (mixture of 56 % KOH aqueous solution and DMSO/DMF) according to Scheme 1. The phosphine **1** was obtained by Redmore¹⁴ but phosphines **2** and **3** were first synthesized by reduction of corresponding phosphonates with LiAlH_4 , using standard procedure.^{14b,c}



Scheme 1.

After addition of KOH aqueous solution to starting pyridylphosphines **1-3** in DMF the red colored mixture was observed suggesting the phosphide-anion formation. After slow addition of 1,4-dichlorobutane at 0°C white crystals of KCl precipitated. In the ³¹P NMR spectra of the reaction mixture four signals were registered: triplet at ca. -118 ppm (¹J_{PH} ≈ 205 Hz), doublet at ca. -68 ppm (¹J_{PH} ≈ 210 Hz), doublet at -49 ppm (¹J_{PH} ≈ 210 Hz) and singlet at -11 ppm corresponded to unreacted primary phosphine, mono-substituted product - acyclic secondary phosphine, 1,4-bisphosphinobutanes **7-9** and desired phospholanes **4-6**, respectively. It is interesting to note, that irrespective of ratio between initial phosphine and 1,4-dihalogenalkane the resulting mixture of products was approximately the same.

The mixture of organic products was isolated by hexane extraction, with further solvent and unreacted phosphine

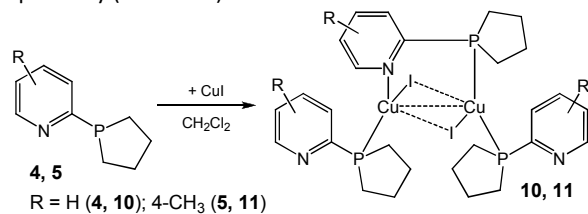
removal under reduced pressure. The crude reaction mixture was separated by fractional distillation in vacuum. The first fraction consisted principally of acyclic secondary monophosphine, the second fraction contained desired pyridine-2-yl-phospholanes **4-6** and distillation residue contained pure 1,4-bis((R-pyridine-2-yl)-phosphino)butanes **7-9**. The novel α,ω -bisphosphinoalkanes **7-9** are high promising starting materials for design of 18-membered macrocycles via covalent self-assembly.¹⁵ ³¹P NMR spectra of pure pyridylphospholanes showed one singlet in the region -11.4 - -12.3 ppm. The ¹H NMR spectra of compounds **4-6** in CDCl₃ showed three groups of signals of cyclic methylene protons – two multiplets at 2.24-2.30 ppm and 1.88-1.98 ppm for P-CH₂ protons, and one multiplet at 1.65-1.75 ppm belonging to cyclic ethylene protons. Pyridyl protons are registered as four groups of signals at 8.58, 7.46, 7.32 and 6.98 ppm (for **4**), three groups of signals at 8.45, 7.22, 6.89 (for **5**) and 7.42, 7.19, 6.92 ppm (for **6**). The signals of methyl protons are found at 2.31 and 2.54 ppm for **5** and **6** respectively.

The obtained phospholanes **4-6** are easily oxidable in air and soluble in most organic solvents.

Synthesis and Structures of Cu(I) complexes. Copper(I) halide complexes exhibit many coordination motifs depending on the coordinating ligand as well as the molar ratios between ligand and metal salt.¹⁶ With pyridine-type ligands L and an equimolar stoichiometry of CuX ($\text{X} = \text{Cl}, \text{Br}, \text{I}$) the complexes frequently form $[\text{CuXL}]_4$ cubane-like structures, one-dimensional ladder chains $[\text{CuXL}]_\infty$ consisting of fused Cu_2X_2 subunits^{1a, 17, 18} or binuclear P,N-complexes of type “head-to-tail”.³ Changing the stoichiometry to a ratio of 1:2 results in a $[(\text{CuX})_2\text{L}_4]$ form of complex with an isolated rhombohedral Cu_2X_2 core.^{1a,c, 19-22} At the ligand-to-metal ratio of 3:2 complexes $[\text{Cu}_2\text{X}_2\text{L}_3]$ with a “butterfly” core were obtained.

We used phospholanes **4-6** as novel type of ligands for the synthesis of Cu(I) complexes. For the complexation reactions, copper(I) iodide was used as metal salt due to its better oxidation stability compared to copper(I) bromide and copper(I) chloride.

The interaction of **4** or **5** and copper (I) iodide in the ratio 3:2 in CH_2Cl_2 led to the formation of complexes **10** and **11** respectively (Scheme 2).



Scheme 2.

Compounds **10** and **11** were obtained as yellow precipitation after reaction mixture concentrating and dropwise addition of ethanol. It should be noted that despite of two types of coordinated ligands (two P-monodentate and one P,N-

bidentate) only one broad singlet at -8.4 ppm (for **10**) or -6.2 ppm (for **11**) is registered in ^{31}P NMR spectra. We suppose that fast exchanging processes between ligand molecules take place in solutions. The ^1H NMR spectra of complexes **10** and **11** in CD_2Cl_2 show only one set of signals: four groups of signals of pyridyl protons at 8.71, 7.66, 7.64 and 7.23 ppm (for **10**) and three groups of signals at 8.46, 7.35, and 6.98 ppm (for **11**), three multiplets of protons for phospholane heterocycle in the region 1.7–2.3 ppm. The signals of pyridyl protons are not significantly shifted relative to the spectra of the initial ligands **4** and **5** which is evidence for the weak coordination of nitrogen atom to metal.

Apart from NMR spectroscopy, complexes **10** and **11** have been characterized by mass-spectrometry and elemental analysis, which also confirmed 3:2 ligand to copper stoichiometry.

The molecular structure of **10** obtained by X-ray diffraction revealed a butterfly-shaped Cu_2I_2 core surrounded by three ligands (Figures 1, S7). Phospholane fragments of all the three ligands adopted chair-like conformation. One of the three ligands acts as bridging unit towards the two copper atoms. The other two ligands coordinate the copper ions only via their phosphorus atom resulting in a tetrahedral coordination for each metal center.

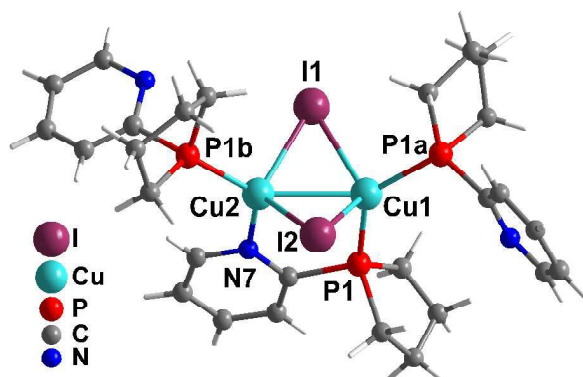
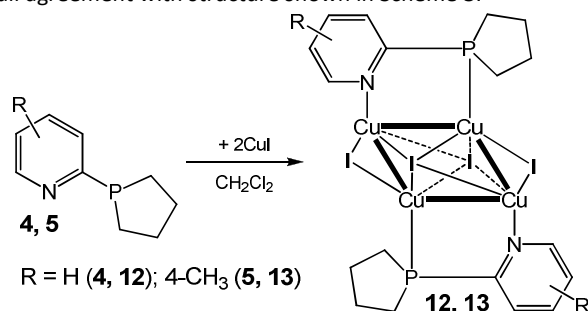


Figure 1. X-Ray molecular structure of complex **10**.

It should be mentioned that a similar structure was reported for luminescent homo- and heteroleptic complexes of diphenylpyrid-2-ylphosphines^{4a,b, 1c} and other N-heterocyclic phosphines.²³ The torsion angle I-Cu-Cu-I expresses the magnitude of the butterfly shape deviation from the usual planar conformation, and for complex **10** it is 141.5°. The copper-copper distance (2.65 Å) is significantly below the sum of the van der Waals radii (2.80 Å)²⁴ and is forced by the close proximity of heteroatoms in the initial ligand like for the previously described butterfly-shaped complexes with P,N- or N,N-ligands.^{4a,b, 23, 25} However, Cu...Cu distance in **10** is shorter than the distance found for their diphenylpyrid-2-ylphosphine and N-heterocyclic phosphine analogues (2.76 – 2.89 Å).^{4a,b, 1c, 23}

The reaction of **4** or **5** with CuI in the ligand-to-metal ratio of 1 : 2 in hot DMF and CH_2Cl_2 led to the formation of tetranuclear

$\text{Cu}_4\text{I}_4\text{L}_2$ complexes **12** and **13** (Scheme 3). Complexes **10**, **11** and **12**, **13** are very different by their solubility in organic solvents: the former two are soluble in the majority of organic solvents, and the latter two are insoluble except in hot DMF. The NMR spectra of **12** and **13** in DMF-d_7 are of similar character and confirm the general similarity of structures. Raman spectra of complexes **12** and **13** show bands that are attributed (on the basis of available literature²⁶ and our DFT computations) to stretching vibrations of pyridyl moieties coordinated to metal centers ($\nu_{\text{pyr,coord}}$) at 1584 and 1601 cm^{-1} , respectively. The stretches of pyridyl moieties free from coordination ($\nu_{\text{pyr,free}}$ = 1577/1591 cm^{-1} in the spectra of ligands **4/5**) are absent, in full agreement with structure shown in Scheme 3.



Scheme 3.

^{31}P NMR spectra show one signal at -5.1 ppm for **12** and -6.6 ppm for **13**. In the ^1H NMR spectra of **12** and **13** all signals of protons of pyridyl fragment and methyl protons of **13** are significantly shifted to low fields relative to the spectra of **4** and **5**, respectively, and registered at 9.05, 8.00, 7.99 and 7.62 ppm (for **12**) and 8.94, 7.93, 7.59 ppm and 2.51 ppm (for **13**) that allows to infer the coordination of pyridyl nitrogen atom to copper.

Complexes **12** and **13** have also been characterized by mass-spectrometry and elemental analysis, which confirmed a 2 : 4 ligand-to-copper stoichiometry.

Crystals of **12** and **13** suitable for single crystal X-ray analysis were obtained by slow cooling of hot DMF solution. Molecular structures of complexes are shown in Figures 2 and S8 (for **12**) and Figure S1 (for **13**) respectively.

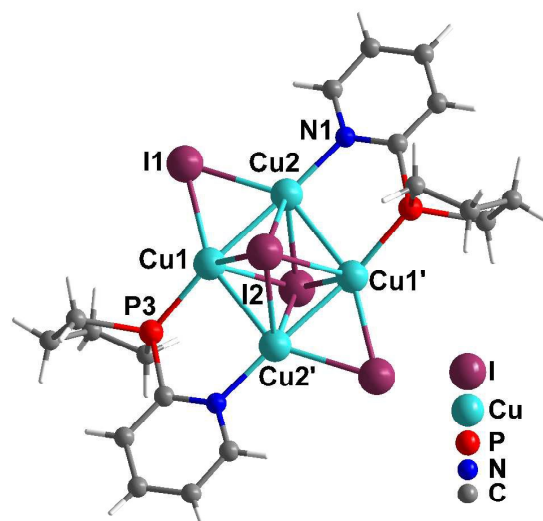


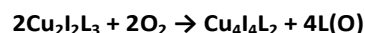
Figure 2. X-Ray molecular structure of complex **12**.

Structure of **12** and **13** represented a tetranuclear complex containing Cu_4I_4 metal-halide core and two molecules of ligand. Unlike the common cubane-like $\text{Cu}_4\text{I}_4\text{L}_4$ clusters the four copper atoms in **12** and **13** are arrayed in a parallelogram with obtuse angle of 96.6° and 96.8° respectively. The Cu_4 array μ^4 -capped by two iodine atoms forms a distorted octahedron, and has two additional iodine atoms μ^2 -bound on each short side of the parallelogram. Two ligand molecules are “head-to-tail” coordinated via both heteroatoms and lie at the long side of Cu_4I_4 parallelogram. The $\text{Cu1}\dots\text{Cu2}$ distance of 2.56 \AA (for **12**) and 2.53 \AA (for **13**) is comparable to equivalent $\text{Cu}\dots\text{Cu}$ distances in known complexes with di(R)-P-(methylpyridyl)phosphines^{5a} and PNP-ligands^{2f} whereas $\text{Cu1}'\text{--Cu2}$ distance of complex **12** (2.67 \AA) is shorter than in complex **13** (2.80 \AA) and P,N-analogues (average $2.83 - 3.03 \text{ \AA}$).

Strong influence of the ligand-to-metal ratio in the complexation reaction on the type of the resulting complexes (vide supra) suggests that kinetic factors play crucial role in the processes of the complex formation. Noteworthy, the transformation of octahedral $\text{Cu}_4\text{I}_4\text{L}_2$ complex into butterfly-like $\text{Cu}_2\text{I}_2\text{L}_2$ complex and *vice versa* during the process of sublimation was observed for complexes of di(R)-P-(methylpyridyl)phosphines.^{5a} According to our quantum-chemical computations at the PBE0-D3/def-TZVP level of theory, the rearrangement of $\text{Cu}_2\text{I}_2\text{L}_2$ complex **10** to $\text{Cu}_4\text{I}_4\text{L}_2$ complex **12** with the release of four ligand molecules **4** is strongly exoenergetic: $\Delta E = 65 \text{ kcal/mol}$. The process results in an increase of entropy of the system, which is reflected in a smaller (relative to ΔE), but still positive free energy of the reaction $\Delta G = 18 \text{ kcal/mol}$. $\Delta E = 72 \text{ kcal/mol}$ and $\Delta G = 26 \text{ kcal/mol}$ are predicted for analogues transformation of complex **11** to complex **13**. Thus, the transformation is unfavourable thermodynamically, and $\text{Cu}_2\text{I}_2\text{L}_2$ complex would

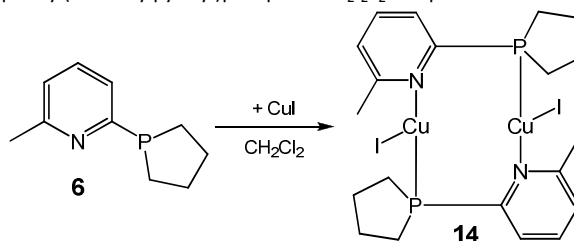
be a major product of the reactions discussed above if thermodynamic factors dominated.

It is interesting that the boiling of “butterfly-like” complexes **10** and **11** in DMF without atmospheric oxygen protection during two hours results in the formation of insoluble complexes **12** and **13** respectively. Moreover, complex **13** was obtained as minor product after a work-up of the reaction mixture of **11**. We suppose that the atmospheric oxygen promotes the transformation according to the following reaction:



Indeed, the ^{31}P NMR spectra of **10** after boiling in hot DMF showed along with signal of Cu-complex **12** the signal of the oxidized ligand ($\delta_{\text{P}} = 61.5 \text{ ppm}$). Our DFT computations demonstrate that the transformation according to the reaction presented above is strongly advantageous both energetically and thermodynamically: $\Delta E' = -166$ and -160 kcal/mol , $\Delta G' = -185$ and -179 kcal/mol for transformations of **10** to **12** and **11** to **13** respectively.

The modification of the ligand by introduction of a methyl group in the 6-position of the pyridyl moiety could lead to a completely different coordination behavior of pyridylphospholane. It is reported that the attempt to obtain “butterfly-like” complex on the basis of diphenyl(6-methyl)pyridylphosphine was unsuccessful and only P-monodentate neutral complex $[\text{CuL}_3]$ was obtained.^{4a} Quite recently the binuclear P,N-coordinated “head-to-tail” complexes $\text{Cu}_2\text{I}_2\text{L}_2$ were synthesized by reaction of diphenyl(6-methyl)pyridylphosphine and copper(I) halides.³ The interaction of 6-methylpyridyl substituted ligand **6** with CuI in the ratio 3:2 in CH_2Cl_2 or in pyridine led to the formation of complex **14** (Scheme 4). According to elemental analysis data and ESI mass-spectra complex **14** contains two ligand molecules and two copper atoms. The structure of **14** is proposed on the basis of the similarity of spectral and photophysical data of recently described analogous diphenyl(6-methylpyridyl)phosphine $\text{Cu}_2\text{I}_2\text{L}_2$ complex.³



Scheme 4.

Complex **14** precipitated in dichloromethane, whereas pyridine was evaporated from the reaction mixture and product was precipitated as microcrystalline powder by addition of ethanol. Complex **14** is insoluble in most organic solvents excluding DMF and pyridine. Both samples (from CH_2Cl_2 or pyridine) have the identical NMR spectra in the solutions and Raman spectra in the solid state. Only bands $\nu_{\text{pyr, coord}}$ at 1589 cm^{-1} are found in the Raman spectra, while

the bands $\nu_{\text{pyr}}^{\text{free}}$ (1578 cm^{-1} in the spectrum of ligand **6**) are absent in full agreement with structure shown in Scheme 5. The ^{31}P NMR spectrum of **14** in DMF-d_7 shows one signal at -9.0 ppm. The signals of pyridyl protons and methyl protons are low-field shifted in comparison to the same signals in the spectrum of **6** ($\Delta\delta \approx 0.5$ ppm and 0.2 ppm respectively), which is evidence for coordination of N-atom of pyridyl substituent to metal center. It should be mentioned that in deuteropyridine the signals of all protons are registered at common fields and it is questionable whether the complexes have the identical molecular structure both in DMF and in pyridine, in particular since the latter is able to compete with pyridyl substituent of phospholane for coordination with copper.

The structure of complex **14** shown in Scheme 4 was optimized quantum chemically (Figure S2, Table S1, ESI), and emission spectra computationally predicted for this structure closely corresponded to the respective experimental spectra (*vide infra*). This should be regarded as an additional proof of the structure deduced on the basis of NMR and Raman spectroscopy and elemental analysis.

Photophysical properties and theoretical characterization. The absorption spectra of free ligand **4** and of complexes **10-14** registered at room temperature are shown in Figure 3.

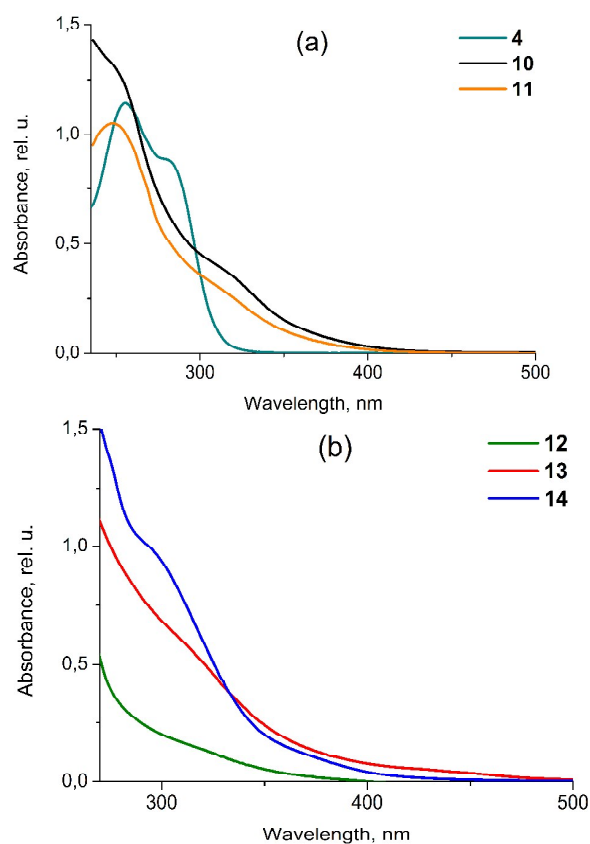


Figure 3. Absorption spectra of (a) free ligand **4** and complexes **10-11** in CH_2Cl_2 ; (b) complexes **12-14** in DMF.

Shoulders at ca. 255 nm in the spectra of all complexes as well as bands at 255 and 281 nm in the free ligand spectrum can be assigned to transitions within the pyridyl rings on the phospholane moieties. The spectra of complexes feature additional bands at ca. 310-320 nm and/or tails ranging from 300 to ca. 480 nm, absent in the free ligands spectra. These low-energy absorptions are assigned to metal-to-ligand charge-transfer (MLCT) transitions mixed with halogen-to-ligand charge-transfer (XLCT) transitions and therefore belong to (X+M)LCT states. Quite similar spectra were reported for closely related diphenylphosphinopyridines and the corresponding $\text{Cu}_2\text{I}_2\text{L}_2$ and $\text{Cu}_4\text{I}_4\text{L}_2$ complexes.^{4a,c,5a}

The above preliminary interpretation of the absorption spectra is fully supported by quantum chemical TD-DFT calculations at CAM-B3LYP/def-TZVP level of approximation. Calculated spectra of compounds **4** and **10-14** are presented at Figure S3 and S5, ESI. The computations reproduce qualitatively the main differences in the experimental spectra of ligands and complexes. The low-energy bands at ca. 320-370 nm in the simulated spectra of complexes **10-14** result from transitions between frontier molecular orbitals (FMOs), some of which are shown in Figure 4. The highest occupied molecular orbitals (HOMOs) reside on the Cu_nI_n core and the lowest unoccupied molecular orbitals (LUMOs) are located on the ligands. Thus, the bands are attributed to (M+X)LCT transitions. High-energy bands at ca. 280 and ca. 260 nm should be assigned to intraligand transitions of mixed $n-\pi^*$ and $\pi-\pi^*$ character (see Figures S3, S4, ESI, for details).

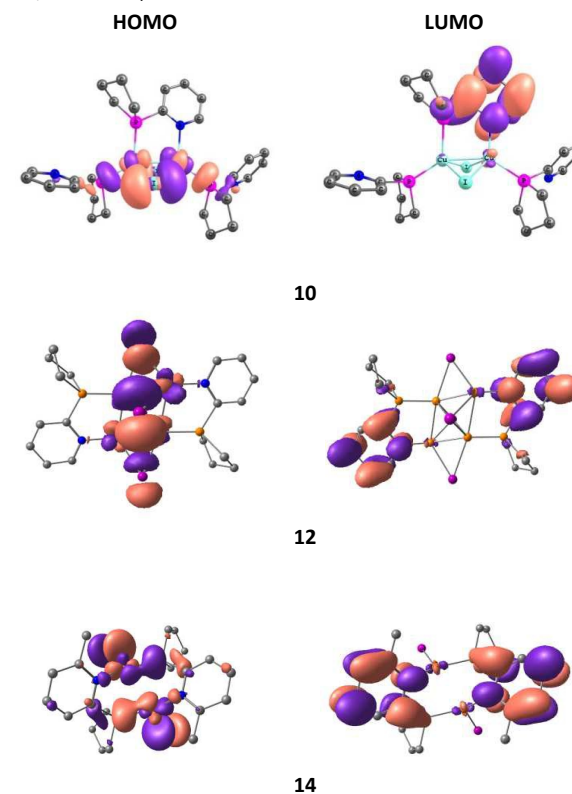


Figure 4. HOMO (left) and LUMO (right) of complexes **10** (a), **12** (b) and **14** (c).

The solid-state emission spectra at room temperature of complexes **10-14** shown in Figure 5 differ for each type of complex, while solid state excitation spectra resemble each other and demonstrate one broad feature from 310 to 400 nm with maxima at 357, 364, 342, 390 and 367 nm for complexes **10-14**, respectively. Stokes shifts of the emission maxima of **10-14** (ca. 150-200 nm) and excited state lifetimes in the microsecond domain indicate the triplet origin of the observed emission.

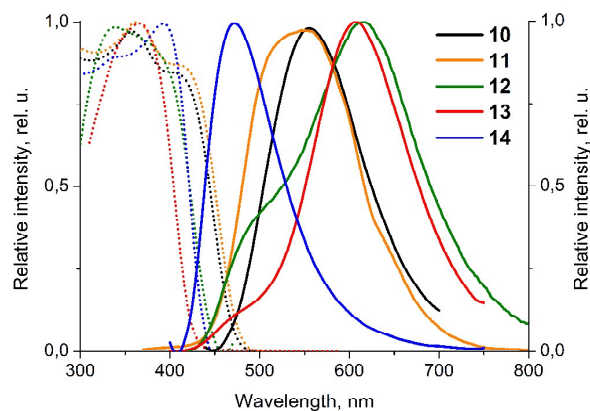


Figure 5. Solid state excitation (dotted) and emission spectra of complexes **10-14** at 300K.

Complexes **10** and **11** demonstrate true green emission with the maximum of a band in the spectra at 555 and 550 nm, respectively that is typical for “butterfly-like” binuclear complexes based on the pyridylsubstituted phosphine ligands which, on the whole, were reported to emit light in the range 497 – 552 nm.^{4a,b, 23} The emission maxima (537 and 523 nm, respectively)^{4a} for complexes of diphenylphosphinopyridine ligands most closely related to complexes **10** and **11** are slightly blue-shifted compared to the latter. The emission of complex **14** is significantly blue-shifted compared to **10** and **11** and demonstrates maximum at 471 nm, similar to the case reported for analogous complex of pyridyldiphenylphosphine, where the emission was observed at 485 nm.³ This experimental trend is nicely reproduced by our TD-DFT computations: there is a linear correlation between the experimental positions of the emission maxima with TD-DFT computed wavelengths for $T_1 - S_0$ transitions (Figure 6). Good quality of the correlation should be regarded as a confirmation of correctness of the quantum-chemically optimized (at the UPBE0-D3/def-TZVP level) structures of complexes **11** and **14** deduced on the basis of spectroscopic methods and elemental analysis.

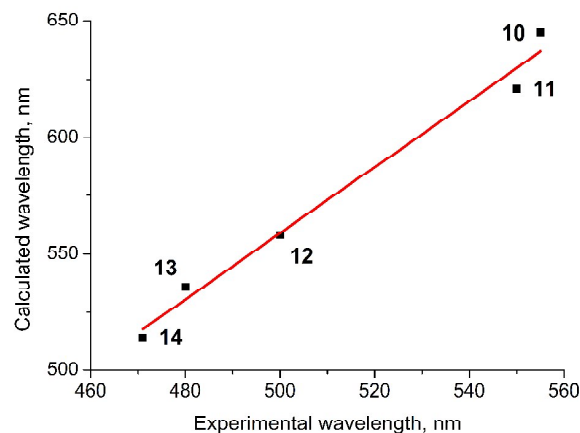


Figure 6. Correlation between TD-DFT computed wavelengths of $T_1 - S_0$ transitions and experimental positions of emission maxima of complexes **10-14**. Only experimental positions of high-energy bands were taken into account for complexes **12** and **13** (vide infra).

Our DFT computations show that FMOs of optimized triplet-state structures of complexes **10** and **11** are very similar to the corresponding orbitals of the ground state shown in Figure 4 (a). Thus, the emission bands resulting from a vertical transition between these orbitals can be interpreted as being of $^3(X+M)$ LCT character, similar to the corresponding absorption bands (vide supra).

In the emission spectra of octahedral complexes **12** and **13** two bands are observed: high-energy (HE) band at 490-500 nm and low-energy (LE) band at 600-615 nm. Recently it was shown that analogous octahedron tetranuclear copper-iodine complex of di(R)-P-(methylpyridyl)phosphines demonstrated dual emission at the range of 450-470 and 560-580 nm, respectively, which was explained by the effects of unequal Cu–Cu bonds length and by the rigid coordination environment enforced by the bidentate P^{AN} ligands.^{5a} To shed light on the observed dual emission of complex **12**, we performed a DFT analysis of the FMOs of this molecule. Quantum-chemical studies of this kind have proven to be helpful in establishing the nature of the HOMO and LUMO of related copper complexes and aided in the assignment of spectral transitions.²⁷ Frontier molecular orbitals (FMOs) of complex **12** calculated for the singlet ground state S_0 are shown in Figure 4: the HOMO is mainly localized on Cu_4I_4 core, while the LUMO is almost exclusively on the pyridyl groups. The contribution of the atomic orbitals of iodine, copper, carbon and nitrogen atoms is similar to that described for cubane $[Cu_4I_4(pyridine)_4]$ cluster.^{27a} At the S_0 state minimum-energy geometry, the 26 upper HOMOs are combinations of copper d and iodine p orbitals, with pyridine-based bonding orbitals lying at lower energies (Figure S6, ESI). The four LUMOs of lowest energy are π^* orbitals of the pyridine moieties. The LUMO+4 represents mainly a combination of copper (66%) and iodine (18%) s-p states. The HOMO remains of qualitatively the same character for the triplet state: 41% on I ions, 40% on Cu ions, while LUMO is contributed by both Cu_4I_4 core (15% on I ions and 37% on Cu ions) and pyridyl (37%) moieties (Figure 7). This, as well as quite moderate

perturbation of the complex geometry after the singlet-triplet excitation, allows to interpret the HE triplet-singlet transition as being predominantly of $^3(X+M)LCT$ character on analogy with the results of De Angelis et al.,^{27a} though with admixture of cluster centered (3CC) character. This suggests that LE emission, which by analogy with the results of De Angelis et al.^{27a} could be assigned to vertical transition from a different triplet state, is mainly of 3CC character, though a minor admixture of $^3(X+M)LCT$ state cannot be excluded.

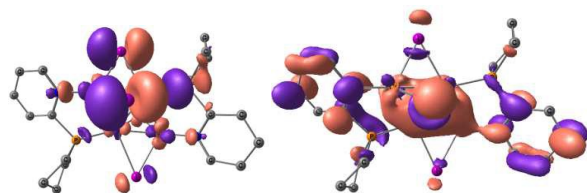


Figure 7. HOMO (left) and LUMO (right) of ground singlet state of complex **12** computed on the optimized triplet-state structure.

Emission quantum yields for complexes **10-14** are in the range of 1-28 %, the highest quantum yield (28%) being observed for the octahedral complex **12**. They are comparable to the values found for similar binuclear as well as tetranuclear complexes.^{4a, 5a}

It should be mentioned that octahedron tetranuclear complexes **12** and **13** demonstrate thermochromic effects in the solid state, which can be observed even with the naked eye. These Cu_4I_4 complexes demonstrate nearly white emission at room temperature, while the cooling of the samples by the liquid nitrogen gives the blue emission under the UV-light. Low temperature experiments at 77K demonstrate the quenching of the low-energy transitions and disappearance of the band at 600 nm, while the stepwise increasing of the temperature gives the increasing of LE-transition and quenching of HE-transitions.

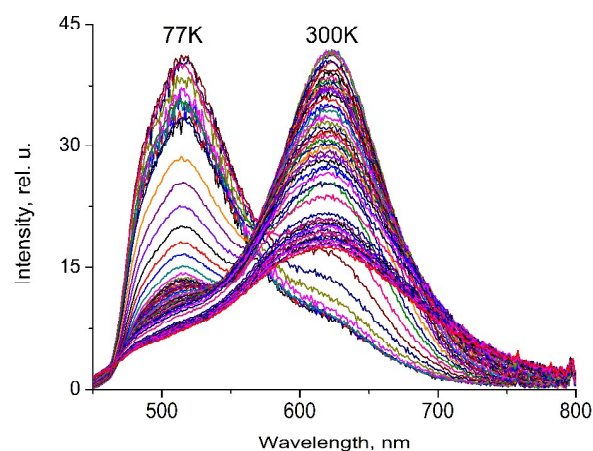


Figure 8. Solid state emission spectra of complex **12** in the range of temperatures 77-300K.

This thermochromic response of complex **12**, connected with the nuclear motion impediment at low temperature, is similar to cubane $Cu_4I_4L_4$ clusters,^{27a} which supports our interpretation of the

LE band as being of 3CC character (vide supra) with significantly distorted Cu_4I_4 core in the corresponding triplet state.

Conclusions

In summary, copper(I) complexes based on five-membered heterocyclic pyridylphospholane ligands exhibit a high structural diversity. Dinuclear complexes **10** and **11** with stoichiometry $Cu_2I_2L_3$ are obtained using phospholane ligands with pyridine-2-yl- and 4-methylpyridine-2-yl substituents at phosphorus atom. Additionally tetranuclear complexes $Cu_4I_4L_2$ **12** and **13** can be synthesized by reacting of above mentioned ligands with copper iodide in a 1 : 2 stoichiometry or by thermal rearrangement of **10** and **11** on air. However, only the dinuclear bisligand “head-to-tail” complex $Cu_2I_2L_2$ is formed by the reaction of 1-(6-methylpyridine-2-yl)phospholane with CuI . The structural diversity of the obtained complexes is reflected in their photophysical properties: the compounds show phosphorescence in the broad spectral range of 471 – 615 nm, which overlaps only partially with previously reported luminescence for similar copper iodide complexes with pyridilphosphines (450-580 nm).

Experimental

All reactions and manipulations were carried out under a dry argon atmosphere by using standard vacuum-line techniques. Solvents were purified, dried, deoxygenated, and distilled before use. EI-MS (70 eV) were recorded with a DFS Thermo Electron Corporation (Germany) spectrometer with direct sample admission into the ion source (ion-source temperature = 2808°C; vaporizer temperature programmed from 50–3508°C). The XCalibur program was used to process the mass spectrometry data. The mass spectra are reported as m/z values with relative intensities (I_{rel}) [%]. 1H NMR (400 MHz and 500 MHz) and ^{31}P NMR (162 and 242 MHz) spectra were recorded with a Bruker Avance-DRX 400 and Bruker Avance-500 spectrometers. Chemical shifts are reported in ppm relative to $SiMe_4$ (1H , internal standard), and 85% H_3PO_4 (aq) (^{31}P ; external standard). Coupling constants (J) are reported in Hz.

Determination of CHN content was carried out on CHN analyzer “CHN-3 KBA”. Determination of phosphorus content was provided by combustion in an oxygen stream and for iodine determination an analysis via Shoniger titration was used.

O,O-Diethyl(pyrid-2-yl)phosphonate was obtained from pyridine-N-oxide and sodium diethylphosphonate by an improved Redmors method.¹⁴ 2-Pyridylphosphine **1** was obtained from O,O-diethyl(pyrid-2-yl)phosphonate by reduction with $LiAlH_4$ in diethyl ether using known method.^{14b,c}

Photophysical Measurements. UV/VIS spectra were registered at room temperature on a PERKIN-ELMER LAMBDA 35 spectrometer with a scan speed of 480 nm/min, using a spectral width of 1 nm. All samples were prepared as solutions in dichloromethane (**4**, **10**, **11**) and dimethylformamide (**12-14**) with the concentrations of $ca. 10^{-5}$ mol/l and placed in 10 mm quartz cells. Excitation and emission

spectra for solid-state samples at room temperature and at 77K were measured on Fluorolog 3 (Horiba Jobin Yvon) spectrofluorimeter of the Center for optical and laser materials research of Saint-Petersburg State University. Powder samples were supported on the quartz glass plates. LED (maximum of emission at 265 nm, 340 nm and 390 nm) were used in pulse mode to pump luminescence in lifetime measurements (pulse width 0.9 ns, repetition rate 100 Hz to 10 kHz). The integration sphere was used to measure the solid state emission quantum yield for the complexes **10-14**. Raman spectra were registered at room temperature on a BRUKER RAM II module (using a Ge detector operating at liquid nitrogen temperature) attached to a BRUKER VERTEX 70 FTIR spectrometer in the range 10-4000 cm^{-1} with an optical resolution of 4 cm^{-1} . Raman scattering radiation was collected in a back-scattering configuration. 1024 scans were averaged for each spectrum. A Nd:YAG laser with a wavelength of 1064 nm and power of 150-250 mW was used as the excitation source. The samples were inserted in a standard glass cell.

Computational Methods. Quantum chemical calculations were performed with the TURBOMOLE 6.4²⁸ and the Gaussian-03²⁹ suites of programs. The hybrid PBE0 functional³⁰ and the Ahlrichs' triple- ζ def-TZVP AO basis set³¹ were used for optimization of all structures. Stationary points were characterized as minima by frequency analyses. The same frequencies were used in the computations of the free energy.³² In all geometry optimizations the RI-JK approximation³³ for the two-electron integrals (with accompanying auxiliary basis set taken from the TURBOMOLE basis set library³¹) and the D3 approach³⁴ to describe the London dispersion interactions together with the Becke-Johnson (BJ) damping function³⁵ were employed as implemented in the TURBOMOLE program. Time-Dependent Density Functional Response Theory (TD-DFT)³⁶ has been employed to compute the vertical excitation energies (i.e., absorption wavelengths) and oscillator strengths for the ground-state optimized geometries in the gas phase. Using Gaussian, 50 lowest singlet excited states were taken into account. The procedure was analogous to the one described elsewhere,³⁷ except that the range-separated CAM-B3LYP functional was used instead of PBE0. Calculated spectra were convoluted with a Lorentzian lineshape function (f.w.h.m. = 0.25 eV) and shifted by -0.24 eV. The vertical $T_1 - S_0$ transition energies were also computed at CAM-B3LYP/def-TZVP level. Percent contributions of atoms/atom group to molecular orbitals were calculated with GaussSum program.³⁸

X-Ray Crystallography. Data of **10**, **12** and **13** were collected on a Bruker Smart Apex II CCD diffractometer using graphite monochromated $\text{MoK}\alpha$ ($\lambda = 0.71073 \text{ \AA}$) radiation and ω -scan rotation. Data collection images were indexed, integrated, and scaled using the APEX2 data reduction package³⁹ and corrected for absorption using SADABS⁴⁰. The structure was solved by direct methods and refined using SHELX⁴¹ program. All non-hydrogen atoms were refined anisotropically. H atoms were calculated on idealized positions and refined as riding atoms. Figures 1, 2 and S1 were generated by DIAMOND Version 3.2K (copyright Crystal

Impact GbR), Figures S7 and S8 were generated by ORTEP for Windows⁴¹.

CCDC 1420908 (**10**), 1420907 (**12**), 1429275 (**13**) contain the supplementary crystallographic data for this paper. These data can be obtained free of charge via www.ccdc.cam.ac.uk/conts/retrieving.html (or from the Cambridge Crystallographic Data Centre, 12 Union Road, Cambridge CB2 1EZ, UK; fax: (+44) 1223-336-033; or deposit@ccdc.cam.ac.uk).

Crystal data of 10. $\text{C}_{27}\text{H}_{36}\text{Cu}_2\text{I}_2\text{N}_3\text{P}$, $M = 876.38$, $T = 293 \text{ K}$, $a = 11.951(4)$, $b = 18.183(7)$, $c = 15.128(5) \text{ \AA}$, $\beta = 102.604(4)^\circ$, $V = 3208(2)$, space group $P2_1/n$ (no. 14), $Z = 4$, 37287 reflections measured, 7670 unique ($R_{\text{int}} = 0.0647$) which were used in all calculations. The final $wR(F_2)$ was 0.1601 (all data).

Crystal data of 12. $\text{C}_{18}\text{H}_{28}\text{Cu}_4\text{I}_4\text{N}_2\text{P}_2$, $M = 1092.13$, $T = 150 \text{ K}$, monoclinic, triclinic, $a = 9.0224(8)$, $b = 9.4377(8)$, $c = 9.4869(8) \text{ \AA}$, $\alpha = 66.6150(10)$, $\beta = 102.604(4)$, $\gamma = 64.3900(10)^\circ$, $V = 667.24(10)$, space group $P-1$ (no. 2), $Z = 1$ (molecule in special position), 5279 reflections measured, 2595 unique ($R_{\text{int}} = 0.0210$) which were used in all calculations. The final $wR(F_2)$ was 0.0949 (all data).

Crystal data of 13. $\text{C}_{20}\text{H}_{28}\text{Cu}_4\text{I}_4\text{N}_2\text{P}_2$, $M = 1120.14$, $T = 296 \text{ K}$, monoclinic, $a = 9.662(5)$, $b = 17.858(8)$, $c = 9.108(5) \text{ \AA}$, $\alpha = 90$, $\beta = 105.994(9)$, $\gamma = 90^\circ$, $V = 1511(2)$, space group $P2_1/c$ (no. 14), $Z = 2$, 6563 reflections measured, 2958 unique ($R_{\text{int}} = 0.1350$) which were used in all calculations. The final $wR(F_2)$ was 0.4329 (all data).

Typical experimental procedure for the synthesis of 4-methyl pyridine-2-yl phosphine (**2**) and 6-methyl pyridine-2-yl phosphine (**3**).

To suspension of lithium tetrahydroaluminate (160 mmol, 200 mmol) in diethyl ether at -2°C solution of O,O-dialkyl(*n*-methylpyridine-2-yl)phosphonate (110 mmol, 130 mmol) was added dropwise. Color of reaction mixture changed from grey to orange. Reaction mixture was stirred 16 h at room temperature. After that 60 ml of degassed water was added dropwise and grey precipitate was occurred and reaction mixture divided to layers. Organic layer was separated, residuary products were extracted with diethyl ether (3x30 ml) from aqueous layer. Organic layer was dried over MgSO_4 . Solvent was removed by distillation, residue was separated by fractional distillation under reduced pressure.

2. Yield 8.4g (52 %). b.p. $101-103^\circ\text{C} / 20 \text{ Torr}$. $^1\text{H NMR}$ (CDCl_3): δ_{H} 8.41 (d, $^3J_{\text{HH}} = 5.1 \text{ Hz}$, 1H, Py-6), 7.31 (s, 1H, Py-3), 6.94 (dm, $^3J_{\text{HH}} = 5.1 \text{ Hz}$, 1H, Py-5), 4.08 (d, $^3J_{\text{HH}} = 204 \text{ Hz}$, 2H, PH), 2.28 (s, 3H, CH_3). $^{31}\text{P NMR}$ (CDCl_3): $\delta_{\text{P}} -119.1 \text{ ppm}$ (t, $^1J_{\text{PH}} = 204 \text{ Hz}$).

3. Yield: 7.56 g (55%). b.p. $61-63^\circ\text{C} / 15-20 \text{ Torr}$. $^1\text{H NMR}$ (CDCl_3): δ_{H} 7.42 (ddd, $^3J_{\text{HH}} = 7.5 \text{ Hz}$, $^3J_{\text{HH}} = 7.8 \text{ Hz}$, $^4J_{\text{HH}} = 2.3 \text{ Hz}$, 1H, Py-4), 7.29 (d, $^3J_{\text{HH}} = 7.5 \text{ Hz}$, 1H, Py-5), 6.99 (d, $^3J_{\text{HH}} = 7.8 \text{ Hz}$, 1H, Py-3), 4.11 (d, $^1J_{\text{PH}} = 204 \text{ Hz}$, 2H, PH), 2.53 (s, 3H, Py- CH_3). $^{31}\text{P NMR}$ (CDCl_3): $\delta_{\text{P}} -118.8 \text{ m.d.}$ (t, $^1J_{\text{PH}} = 204 \text{ Hz}$).

Typical experimental procedure for synthesis of phospholanes **4-6**

To solution of corresponding primary phosphine (**1-3**) (40 mmol) in DMF (40 ml) 56 % aqueous solution of KOH (80 mmol) was added dropwise. After 2 h reaction mixture was cooled to 3°C and 1,4-dichlorobutane (40 mmol) in DMF (30 ml) was added dropwise in 1 h. Mixture was allowed to room temperature and stirred overnight. Degassed water (40 ml) was added, organic layer was separated via

canula, resudary products were extracted with n-hexane (3x30 ml) from aqueous layer. Organic layer was dried over MgSO₄. Solvent was removed by distillation, residue was separated by fractional distillation under reduced pressure.

1-(pyridine-2-yl)-phospholane 4. Yield 1.99 g (30%); b.p. 51-54 °C/0.03 Torr. ¹H NMR (CDCl₃) δ_H 8.58 (ddd, ³J_{HH} = 4.8 Hz, ⁴J_{HH} = 1.7 Hz, ⁵J_{HH} = 1.1 Hz, 1H, Py-6), 7.46 (dddd, ³J_{HH} = 7.7 Hz, ³J_{HH} = 7.5 Hz, ⁴J_{HH} = 1.7 Hz, ⁵J_{HH} = 1.1 Hz, 1H, Py-4), 7.32 (dddd, ³J_{HH} = 7.7 Hz, ³J_{PH} = 2.1 Hz, ⁴J_{HH} = 1.1 Hz, ⁵J_{HH} = 1.1 Hz, 1H, Py-3), 6.98 (dddd, ³J_{HH} = 7.7 Hz, ³J_{HH} = 4.8 Hz, ⁵J_{HH} = 1.1 Hz, ⁴J_{PH} = 0.6 Hz, 1H, Py-5), 2.16-2.25 (m, 2H, P-CH_A), 1.78 - 1.95 (m, 2H, P-CH_B), 1.56-1.71 (m, 4H, H-2). ³¹P NMR (CDCl₃): δ_P -11.4.

Distillery slop contained **1,4-bis(pyridine-2-yl-phosphino)butane 7.** Yield 1.58 g (29 %). ¹H NMR (CDCl₃) δ_H 8.53 (d, ³J_{HH} = 6.3 Hz, 2H, Py-6); 7.46 (dddd, ³J_{HH} = 7.70 Hz, ³J_{HH} = 7.5 Hz, ⁴J_{HH} = 1.92 Hz, 2H, Py-4); 7.35 (bd, ³J_{HH} = 7.7 Hz, 2H, Py-5), 7.04 (dd, ³J_{HH} = 7.5 Hz, ³J_{HH} = 4.9 Hz, 2H, Py-3), 4.14 (ddd, ¹J_{PH} = 210 Hz, ³J_{HH} = 8.3 Hz, ³J_{HH} = 6.2 Hz, 2H, P-H); 1.89-2.00 (m, 2H, P-CH_A), 1.71-1.82 (m, 2H, P-CH_B); 1.44-1.56 (m, 4H, C-(CH₂)₂-C). ³¹P NMR (CDCl₃): δ_P -49.1 (¹J_{PH} = 210.3 Hz), -49.1 (¹J_{PH} = 211.3 Hz).

1-(4-methylpyridine-2-yl)-phospholane 5. Yield: 2.79 g (39%); b.p. 83-85 °C/0.015 Torr. ¹H NMR (500 MHz, CDCl₃): δ_H 8.45 (d, ³J_{HH} = 6.3 Hz, 1H, Py-6); 7.22 (bs, 1H, Py-3); 6.89 (dm, ³J_{HH} = 6.3 Hz, 1H, Py-5); 2.31 (s, 3H, CH₃); 2.23-2.28 (m, 2H, H-1_A); 1.87-2.00 (m, 2H, H-1_B); 1.68-1.76 (m, 4H, H-2). ³¹P NMR (CDCl₃): δ_P -12.0 ppm.

Distillery slop contained **1,4-bis(4-methyl-pyridine-2-yl-phosphino)butane 8.** Yield: 1.64 g (27%). ¹H NMR (400 MHz, CDCl₃): δ_H 8.46 (d, ³J_{HH} = 6.3 Hz, 2H, Py-6); 7.26 (bs, 2H, Py-3); 6.94 (d, ³J_{HH} = 6.3 Hz, 2H, Py-5); 4.18 (ddd, ¹J_{PH} = 210 Hz, ³J_{HH} = 8.1 Hz, ³J_{HH} = 6.3 Hz, 2H, P-H); 2.3 (s, 6H, CH₃); 2.05-1.97 (m, 2H, P-CH_A); 1.88-1.76 (m, 2H, P-CH_B); 1.60-1.54 (m, 4H, C-(CH₂)₂-C). ³¹P NMR (CDCl₃): δ_P -49.3 (¹J_{PH} = 210.3 Hz), -49.9 (¹J_{PH} = 211.3 Hz).

1-(6-methylpyridine-2-yl)-phospholane 6. Yield: 2.08 g (29%); b.p. 72-74 °C/0.03 Torr. ¹H NMR (500 MHz, CDCl₃): δ_H 7.42 (dm, ³J_{HH} = 7.7 Hz, 1H, Py-4), 7.19 (ddd, ³J_{HH} = 7.7 Hz, ⁴J_{HH} = 3.85 Hz, ³J_{PH} = 2.15 Hz, 1H, Py-3), 6.92 (dm, ³J_{HH} = 7.7 Hz, 1H, Py-5), 2.54 (s, 3H, CH₃), 2.24-2.3 (m, 2H, H-1_A), 1.86-1.96 (m, 2H, H-1_B), 1.65-1.71 (m, 4H, H-2). ³¹P NMR (CDCl₃): δ_P -12.3 ppm.

Distillery slop contained **1,4-bis(6-methyl-pyridine-2-yl-phosphino)butane 9.** Yield: 1.59 g (26%). ¹H NMR (400 MHz, CDCl₃): δ_H 7.43 (ddd, ³J_{HH} = 7.7 Hz, ⁴J_{HH} = 5.45 Hz, ³J_{PH} = 2.2 Hz, 2H, Py-4); 7.24 (dm, ³J_{HH} = 7.8 Hz, 2H, Py-3); 6.90 (dm, ³J_{HH} = 7.58 Hz, 2H, Py-5); 4.18 (ddd, ¹J_{PH} = 211 Hz, ³J_{HH} = 8.12 Hz, ³J_{HH} = 6.41 Hz, 2H, P-H); 2.54 (s, 6H, CH₃); 2.04-1.97 (m, 2H, P-CH_A); 1.87-1.79 (m, 2H, P-CH_B); 1.60-1.56 (m, 4H, C-(CH₂)₂-C). ³¹P NMR (CDCl₃): δ_P -49.5 (¹J_{PH} = 210.9 Hz), -49.9 (¹J_{PH} = 211 Hz).

Synthesis of Complex 10. To a solution of **4** (0.3 g, 1.57 mmol) in dichloromethane (3 ml) the suspension of copper (I) iodide (0.29 g, 1.57 mmol) in dichloromethane (5 ml) was added. The color of the reaction mixture changed from yellow to brown. Reaction mixture was stirred for 12 h at room temperature. Afterward the solvent was evaporated and complex was purified through precipitation with ethanol (20 ml). The yellow solid was filtered off, washed with ethanol and dried at 0.05 Torr. Yield: 0.32 g (70%); Mp = 136 °C.

¹H NMR (400 MHz, CD₂Cl₂): δ_H 8.71 (d, ³J_{HH} = 4.9 Hz, 1H, Py-6), 7.66 (m, 1H, Py-3), 7.64 (dddd, ³J_{HH} ≈ ³J_{HH} ≈ 7.3, ⁴J_{HH} ≈ ⁴J_{PH} ≈ 2 Hz, 1H, Py-4), 7.23 (dddd, ³J_{HH} = 4.9, ³J_{HH} = 7.3, ⁴J_{HH} ≈ ⁵J_{PH} ≈ 2 Hz, 1H, Py-5), 2.21-2.29 (m, 2H, H-1_A), 2.11-2.20 (m, 2H, H-1_B), 1.78-1.87 (m, 4H, H-2). ³¹P NMR (CD₂Cl₂) δ_P -8.4 (br.s). MS (ESI_{pos}, m/z (I_{rel}, %), ion): 748 (51, [3L+2Cu+I]⁺), 584 (63, [2L + 2Cu + I]⁺), 393 (100, [2L + Cu]⁺). Anal. Calcd. for C₂₇H₃₆N₃P₃Cu₂I₂ [876]: C, 37.00; H, 4.14; Cu, 14.50; I, 28.96; N, 4.79; P, 10.60%. Found: C, 36.95; H, 4.12; Cu, 14.52; I, 29.01; N, 4.74; P, 10.57%.

Complex **10** was boiled in DMF during 2 hours. Cluster **12** was precipitated after slow cooling of solution to 0°C. Pale yellow crystals were collected and dried at low pressure. Yield: 62 %. Mp = 216 °C. ¹H NMR (400 MHz, DMF-d₇): δ_H 9.05 (d, ³J_{HH} = 4.5 Hz, 1H, Py-6), 8.00-8.03 (m, 1H, Py-3), 7.99 (dd, ³J_{HH} ~ ³J_{HH} ≈ 7 Hz, 1H, Py-4), 7.62 (dd, ³J_{HH} + ³J_{HH} ≈ 11.5 Hz, 1H, Py-5), 2.25-2.34 (m, 2H, P-CH_A), 2.23-2.15 (m, 2H, P-CH_B), 1.85-2.03 (m, 4H, H-2). ³¹P NMR (400 MHz, DMF-d₇): -5.1 ppm. MS (ESI_{pos}, m/z (I_{rel}, %), ion): 748 (38, [3L+2Cu+I]⁺), 584 (100, [2L + 2Cu + I]⁺), 393 (83 [2L + Cu]⁺). Anal. Calcd. for C₁₈H₂₄N₂P₂Cu₄I₄ [1092]: C, 19.80; H, 2.21; Cu, 23.27; I, 46.48; N, 2.56; P, 5.67%. Found: C, 19.76; H, 2.20; Cu, 23.47; I, 46.73; N, 2.49; P, 5.62%

Synthesis of Complex 11. To a solution of 1-(4-methylpyridine-2-yl)-phospholane **5** (0.3 g, 1.67 mmol) in dichloromethane (10 ml) copper (I) iodide (0.21 g, 1.1 mmol) was added. Color of reaction mixture changed to dark red. Reaction mixture was stirred for 12 h. The solvent was partially evaporated and complex **13** was precipitated after the addition of ethanol (20 ml). The orange solid was filtered off, washed with ethanol and dried at 0.05 Torr. Yield of **13**: 0.14 g, 45%. Mp = 282 °C. ¹H NMR (500 MHz, DMF-d₇): δ_H 8.94 (d, ³J_{HH} = 5.4 Hz, 1H, Py-6), 7.93 (s, 1H, Py-3), 7.59 (d, ³J_{HH} = 5.4 Hz, 1H, Py-5), 2.08 (s, 3H, CH₃), 2.40 (ddd, ²J_{HH} = 14.9, ²J_{PH} / ³J_{HH} = 7.7/7.3 Hz, 2H, P-CH_{2A}), 2.33 (ddd, ²J_{HH} = 14.9, ²J_{PH} / ³J_{HH} = 7.4/6.7 Hz, 2H, P-CH_{2B}), 2.08 - 2.17 (m, 2H, CH₂), 1.95 - 2.03 (m, 2H, CH₂). ³¹P NMR (162 MHz, DMF-d₇): δ_P -6.6. MS (ESI_{pos}, m/z (I_{rel}, %), ion): 611 (100, [2L+4Cu]⁺), 790 (39, [3L + 2Cu + I]⁺), 993 (19, [M - I]⁺). Anal. Calcd. for C₂₀H₂₈Cu₄I₄N₂P₂ [1120]: C, 21.44; H, 2.52; Cu, 22.69; I, 45.31; N, 2.50; P, 5.53. Found: C, 21.23; H, 2.60; Cu, 22.75, N, 2.43, P, 5.65. The filtrate was evaporated and complex **11** was precipitated from diethyl ether. Yield of **11**: 0.14 g, 28%. Mp = 163 °C. ¹H NMR (500 MHz, CD₂Cl₂): δ_H 8.46(d, ³J_{HH} = 4.8 Hz, 1H, Py-6), 7.35 (s, 1H, Py-3), 6.98 (d, ³J_{HH} = 4.9 Hz, 1H, Py-5), 2.24 (s, 3H, CH₃), 2.18-2.23 (m, 2H, P-CH₂, partially overlapped by signal of CH₃-group), 2.01 - 2.10 (m, 2H, P-CH₂), 1.70 - 1.81 (m, 4H, CH₂). ³¹P NMR (162 MHz, CD₂Cl₂): δ_P -6.2 (s). MS (ESI_{pos}, m/z (I_{rel}, %), ion): 421 (100, [2L+Cu]⁺), 611 (39, [2L + 2Cu + I]⁺), 790 (49, [3L + 2Cu + I]⁺). Anal. Calcd. for C₃₀H₄₂Cu₂I₂N₃P₃ [918]: C, 39.23; H, 4.61; Cu, 13.84; I, 27.63; N, 4.57; P, 10.12%. Found: C, 39.01; H, 4.54; Cu, 13.75, N, 4.64, P, 10.10%.

Synthesis of Complex 13.

To a solution of 1-(4-methylpyridine-2-yl)-phospholane **5** (0.2 g, 1.1 mmol) in dichloromethane (10 ml) copper (I) iodide (0.42 g, 2.2 mmol) was added. Color of reaction mixture changed to brown and in 12 hours the white microcrystalline product precipitated. Complex **13** was filtered off, washed with ethanol and dried at 0.05

Torr. Yield of **13**: 0.41 g (66 %). All spectra are identical to the same for **13** obtained by above described method.

Synthesis of Complex 14. To a solution of 1-(6-methylpyridine-2-yl)-phospholane **6** (0.3 g, 1.67 mmol) in dichloromethane (10 ml) copper (I) iodide (0.21 g, 1.1 mmol) was added. Color of reaction mixture changed from yellow to red. Reaction mixture was stirred for 12 h at room temperature. Complex **14** was obtained as white precipitate. Afterward complex was filtered off, washed with ethanol (10-15 ml) and dried at 0.05 Torr. Yield: 0.25 g, 61 %. Mp = 196 °C. ¹H NMR (400 MHz, DMF-d₇): δ_H 7.90 (ddd, ³J_{HH} = ³J_{HH} = 8.0 Hz, ⁴J_{PH} = 2.0 Hz, 1H, Py-4), 7.75 (br.d, ³J_{HH} = 8.0 Hz, 1H, Py-5/3), 7.47 (d, ³J_{HH} = 7.7 Hz, 1H, Py-5/3), 2.71 (s, 3H, CH₃), 2.25-2.40 (m, 4H, P-CH₂), 1.85 - 2.02 (m, 4H, CH₂). ³¹P NMR (162 MHz, DMF-d₇): δ_P -9.0 (br.s). MS (ESI_{pos}, m/z (I_{rel}, %), ion): 613 (51, [M-I]), 423 (100, [M-Cu-2I]). Anal. Calcd. for C₂₀H₂₈Cu₂I₂N₂P₂ [739]: C, 32.49; H, 3.82; Cu, 17.19; I, 34.33; N, 3.79; P, 8.38%. Found: C, 32.13; H, 3.78; Cu, 17.24; N, 3.68; P, 8.24%.

Acknowledgements

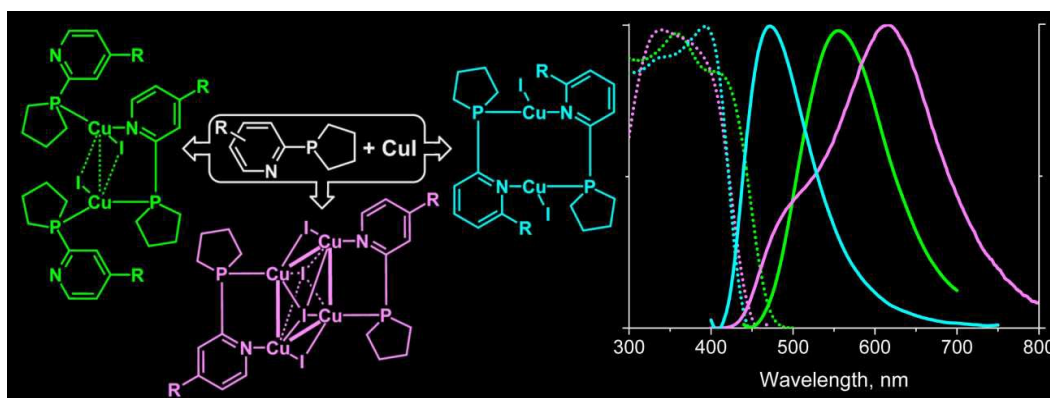
This research has been supported by St. Petersburg State University research grant 12.50.24.2014 and Russian Foundation for Basic Research (grant 14-03-31302_mol_a). The financial support from scholarship programs of the German Academic Exchange Service (DAAD, personal ref. no. 91577762, 91589283) and of the government of the Republic of Tatarstan "Algarish" is gratefully acknowledged (SAK). The work was carried out using equipment of the Center for Optical and Laser Materials Research of St. Petersburg State University.

Notes and references

- (a) P.C. Ford, E. Cariati, J. Bourassa, *Chem. Rev.* 1999, **99**, 3625; (b) H. Xu, R. Chen, Q. Sun, W. Lai, Q. Su, W. Huang, X. Liu, *Chem. Soc. Rev.*, 2014, **43**, 3259; (c) M. Wallesch, D. Volz, D.M. Zink, U. Schepers, M. Nieger, T. Baumann, S. Bräse, *Chem. Eur. J.*, 2014, **20**, 6578
- (a) H. Suh, D.J. Casadonte Jr., L. Hope-Weeks, H.-J. Kim, B. Kim, T. Chang, *Inorg. Chim. Acta*, 2013, **394**, 710, (b) J.-L. Chen, X.-F. Cao, J.-Y. Wang, L.-H. He, Z.-Y. Liu, H.-R. Wen, Z.-N. Chen, *Inorg. Chem.*, 2013, **52**, 9727, (c) L. Bergmann, J. Friedrichs, M. Mydlak, T. Baumann, M. Nieger, S. Bräse, *Chem. Commun.*, 2013, **49**, 6501, (d) L. Zhang, B. Li, Z.J. Su, *J. Phys. Chem. C.*, 2009, **113**, 13968; (e) G.F. Manbeck, W.W. Brennessel, R. Eisenberg, *Inorg. Chem.*, 2011, **50**, 3431; (f) S. Naik, J.T. Mague, M.S. Balakrishna, *Inorg. Chem.*, 2014, **53**, 3864.
- T. Hofbeck, U. Monkowius, H. Yersin, *J. Am. Chem. Soc.*, 2015, **137**, 399
- (a) D.M. Zink, M. Bächle, T. Baumann, M. Nieger, M. Kühn, C. Wang, W. Klopfer, U. Monkowius, T. Hofbeck, H. Yersin, S. Bräse, *Inorg. Chem.*, 2013, **52**, 2292, (b) D. Volz, M. Wallesch, S.L. Grage, J. Göttlicher, R. Steininger, D. Batchelor, T. Vitova, A.S. Ulrich, C. Heske, L. Weinhardt, T. Baumann, S. Bräse, *Inorg. Chem.*, 2014, **53**, 7837; (c) D.M. Zink, T. Baumann, J. Friedrichs, M. Nieger, S. Bräse *Inorg. Chem.* 2013, **52**, 13509.
- (a) Zh. Liu, M.T. Whited, M.E. Thompson, *Inorg. Chem.*, 2012, **51**, 230, (b) D.M. Zink, T. Grab, T. Baumann, M. Nieger, E.C. Barnes, W. Klopfer, S. Bräse, *Organometallics*, 2011, **30**, 3275.
- (a) H. Yersin, A.F. Rausch, R. Czerwieńec, T. Hofbeck, T. Fischer, *Coord. Chem. Rev.* 2011, **255**, 2622, (b) R. Czerwieńec, J. Yu, H. Yersin, *Inorg. Chem.*, 2011, **50**, 8293
- (a) G. Gruttner, M. Wiernik, *Chem. Ber.* 1915, **48**, 1473. (b) G. Gruttner, E. Krause, *Chem. Ber.* 1916, **49**, 437.
- M. J. Burk, *J. Am. Chem. Soc.*, 1991, **113**, 8518
- S.I. Featherman, S.O. Lee, L.D. Quin, *J. Org. Chem.* 1974, **39**, 2899.
- (a) R. Emrich, P.W. Jolly, *Synthesis*, 1993, 39, (b) R.A. Baber, M.F. Haddow, A.J. Middleton, A.G. Orpen, P.G. Pringle, *Organometallics*, 2007, **26**, 713
- (a) E. Vedejs, O. Daugulis, *J. Am. Chem. Soc.*, 1999, **121**, 5813; (b) E. Vedejs, O. Daugulis, *J. Am. Chem. Soc.*, 2003, **125**, 4166
- (a) Ch.J. O'Brien, F. Lavigne, E.E. Coyle, A.J. Holohan, B.J. Doonan, *Chem. Eur. J.*, 2013, **19**, 5854; (b) H. A. van Kalkeren, S.H.A.M. Leenders, C.R.A. Hommersom, F.P.J.T. Rutjes, F.L. van Delft, *Chem. Eur. J.*, 2011, **17**, 11290
- K. Issleib, S. Hausle, *Chem. Ber.*, 1961, 113
- a) D. Redmore, *J. Org. Chem.* 1970, **35**, 4114; b) E.I. Musina, V.V. Khrizanforova, I.D. Strel'nik, M.I. Valitov, Y.S. Spiridonova, D.B. Krivolapov, I.A. Litvinov, M.K. Kadirov, P. Lönnecke, E. Hey-Hawkins, Y.H. Budnikova, A.A. Karasik, O.G. Sinyashin, *Chem. Eur. J.* 2014, **20**, 3169; (c) G. U. Spiegel, O. Stelzer, *Chem. Ber.* 1990, **123**, 989.
- (a) R.N. Naumov, E.I. Musina, K.B. Kanunnikov, T.I. Fesenko, D.B. Krivolapov, I.A. Litvinov, P. Lönnecke, E. Hey-Hawkins, A.A. Karasik, O.G. Sinyashin, *Dalton Trans.*, 2014, **43**, 12784, (b) K.B. Kanunnikov, R.N. Naumov, A.A. Karasik, E. Hey-Hawkins, O.G. Sinyashin, *Phosphor, Sulfur and Silicon and Rel. El.*, 2011, **186**, 888
- D.J. Eisler, C.W. Kirby, R.J. Puddephatt, *Inorg. Chem.*, 2003, **42**, 7626 and references therein.
- K.R. Kyle, C.K. Ryu, J.A. DiBenedetto, P.C. Ford, *J. Am. Chem. Soc.*, 1991, **113**, 2954
- C.M. Fitchett, P.J. Steel, *Inorg. Chem. Commun.*, 2007, **10**, 1297.
- L.M. Engelhardt, P.C. Healy, J.D. Kildea, A.H. White, *Aust. J. Chem.* 1989, **42**, 913.
- J.T. Maeyer, T.J. Johnson, A.K. Smith, B.D. Borne, R.D. Pike, W.T. Pennington, M. Krawiec, A.L. Rheingold, *Polyhedron* 2003, **22**, 419.
- H. Araki, K. Tsuge, Y. Sasaki, S. Ishizaka, N. Kitamura, *Inorg. Chem.* 2005, **44**, 9667.
- C. Hirtenlehner, U. Monkowius, *Inorg. Chem. Commun.* 2012, **15**, 109.
- D.M. Zink, D. Volz, T. Baumann, M. Mydlak, H. Flügge, J. Friedrichs, M. Nieger, S. Bräse, *Chem. Mater.*, 2013, 4471
- A. Bondi, *J. Phys. Chem.* 1964, **68**, 441
- H. Araki, K. Tsuge, Y. Sasaki, S. Ishizaka, N. Kitamura, *Inorg. Chem.*, 2007, **46**, 10032
- J.F. Duncan, K.F. Mok, *Aust. J. Chem.*, 1966, **19**, 701
- (a) F. De Angelis, S. Fantacci, A. Sgamellotti, E. Cariati, R. Ugo, P.C. Ford, *Inorg. Chem.*, 2006, **45**, 10576 and references cited therein; (b) S. Perruchas, C. Tard, X.F. Le Goff, A. Fargues, A. Garcia, S. Kahlal, J.Y. Saillard, T. Gacoin, J. P. Boilot, *Inorg. Chem.*, 2011, **50**, 10682
- TURBOMOLE, a program package developed at the University of Karlsruhe and at the Forschungszentrum Karlsruhe GmbH from 1989 – 2007, and at TURBOMOLE GmbH since 2007; available from <http://www.turbomole.com>
- M.J. Frisch; G.W. Trucks, H.B. Schlegel, G.E. Scuseria, M.A. Robb, J.R. Cheeseman, J.A. Montgomery, T. Vreven, K.N. Kudin, J.C. Burant, et al. Gaussian 03, Revision E.01; Gaussian, Inc.:Wallingford, CT, 2004

- 30 C. Adamo and V. Barone, *J. Chem. Phys.*, 1999, **110**, 6158
- 31 (a) K. Eichkorn, O. Treutler, H. Öhm, M. Häser, R. Ahlrichs, *Chem. Phys. Lett.* 1995, **242**, 652; (b) K. Eichkorn, F. Weigend, O. Treutler, R. Ahlrichs, *Theor. Chem. Acc.*, 1997, **97**, 119; (c) F. Weigend, M. Häser, H. Patzelt and R. Ahlrichs, *Chem. Phys. Lett.*, 1998, **294**, 143
- 32 S. Grimme, *Chem. Eur. J.*, 2012, **18**, 9955
- 33 (a) R. Bauernschmitt, M. Haeser, O. Treutler, R. Ahlrichs, *Chem. Phys. Lett.*, 1997, **264**, 573; (b) R. Bauernschmitt, R. Ahlrichs, *Chem. Phys. Lett.*, 1996, **256**, 454; (c) R. Bauernschmitt, R. Ahlrichs, *J. Chem. Phys.*, 1996, **104**, 9047; (d) J. Wang, R.M. Wolf, J.W. Caldwell, P.A. Kollman, D.A. Case, *J. Comput. Chem.*, 2004, **25**, 1157
- 34 S. Grimme, J. Antony, S. Ehrlich, H. Krieg, *J. Chem. Phys.*, 2010, **132**, 154104
- 35 (a) A.D. Becke, E.R. Johnson, *J. Chem. Phys.*, 2005, **122**, 154104; (b) E.R. Johnson and A.D. Becke, *J. Chem. Phys.*, 2005, **123**, 024101; (c) S. Grimme, S. Ehrlich, L. Goerigk, *J. Comput. Chem.*, 2011, **32**, 1456
- 36 M.E. Casida, In *Recent Advances In Density Functional Methods*; Chong, D. P., Ed.; World Scientific: Singapore, 1995; Vol. 1; pp 155–192
- 37 E.E. Zvereva, S. Grimme, S.A. Katsyuba, T.I. Burganov, A.A. Zagidullin, V.A. Milyukov, O.G. Sinyashin, *J. Phys. Chem. A*, 2013, **117**, 6827
- 38 N.M. O'Boyle, GaussSum 2.0, 2006. Available at <http://gausssum.sf.net>
- 39 APEX2 (Version 2.1), SAINTPlus . Data Reduction and Correction Program (Version 7.31A, Bruker Advanced X-ray Solutions, BrukerAXS Inc., Madison, Wisconsin, USA, 2006.
- 40 G.M. Sheldrick, SADABS, Program for empirical X-ray absorption correction, Bruker-Nonis, 1990 - 2004.
- 41 Sheldrick, G.M. A short history of SHELX SHELX (2008). *Acta Cryst. A* **64**, 112-122

Graphical abstract



Polynuclear Cu(I) complexes with novel type of cyclic phosphine ligands were obtained. Phosphorescence spectra display emission in broad spectral range of 471 – 615 nm.